International Journal of Engineering Research & Technology (IJERT)
ISSN: 2278-0181
Vol. 9 Issue 05, May-2020

Adaptation of A Hydrogen-Enriched Biogas Engine in A Solar-Biogas Hybrid Energy System

Pham Quoc Thai*, Bui Thi Minh Tu
The University of Danang –University of Science and Technology
54 Nguyen Luong Bang str., Danang, Vietnam

***Abstract*—This paper presents the simulated results of the performance and the pollution emission of the hydrogen-enriched biogas engine in the solar-biogas hybrid energy system. This engine is retrofitted from a traditional stationary gasoline engine by adopting an electronic controlled gaseous fuel port injection and variable advance ignition timing. The simulation results reveal that with the same operating conditions and advance ignition angle, the indicative engine cycle work (W_i) and NO_x concentration in the exhaust gas increased as increasing the CH_4 or/and H_2 contents in the fuel mixture. CO and HC concentrations depend mainly on the equivalence ratio. The optimal advance ignition angle decreased as decreasing the load regime or increasing the CH_4 and H_2 contents. A rise in the advance ignition angle results in an increase in NO_x concentration in the exhaust gas. With optimal advance ignition timing, W_i increased by 4%, while NOx concentration rose by 2.5% as shifting from 30% hydrogen-enriched biogas M7C3 fueling mode to neat biogas M7C3 fueling mode. At 70% load regime, the advance ignition angle decreased by 2 degrees as compared to that at full load mode with the same fueling condition.**

***Keywords*—Renewable energy; Biogas; Hydrogen; Solar-Biogas hybrid system; Energy conversion**

NOMENCLATURE

°CA	: Degree of crankshaft angle
MxCy	: Biogas containing 10x% CH_4 and 10y% CO_2 (in volume)
n	: Engine speed (rpm)
SI	: Spark Ignition
T	: Mean temperature of gas mixture in the cylinder (°K)
TDC	: Top Dead Center
W_i	: Indicative engine cycle work (J/cyc)
ϕ	: Global equivalence ratio, ϕ=b
φ	: Crankshaft angle (°CA)
φ_s	: Advance ignition angle (°CA)

I. INTRODUCTION

Climate change has dramatically affected humanity. Vietnam is one of the most affected countries by global warming and sea-level rise. Therefore, we have long been working with the international community to mitigate the rising atmospheric temperature. The country has implemented the strategy of reduction of CO_2 emission according to the roadmap of the Paris Agreement in 2015. As for energy policy, our government has prioritized renewable energy as a source for electricity production. We are increasing electricity generation from renewable sources (excluding hydroelectricity) from 7% in 2020 to 10% from 2030. This will include 2.1% from biomass power, and 3.3% from solar power. This decision is based on our geographical advantage as well as our potential to generate renewable energy.

Regarding the solar power development plan, Vietnam currently has 121 approved solar energy projects added to the national and provincial power plans. The total generating capacity in 2020 is 6.100 MW and up to 7.960 MW in 2030. Besides, there are also 221 projects pending approval with the registered capacity of over 14.330 MW.

Large scale solar power development needs to account for power compensation source, and reserve power source in case of temporary falling down of solar radiation in the daytime or shutting down of solar plant at night. This is one of the difficulties that investors have to deal with when constructing solar power plants. In the past, the problem came from expensive solar cells. But nowadays, on average, solar cell price/cost reduces by half every decade. Therefore, the current challenge is not from cell cost but from dealing with compensation and reserve power source.

A practical solution to cope with this problem is small scale or family-scale solar power production. This approach comprises of using a rooftop solar system/panel supplement with other renewable power sources. This solution neither affects the current electrical grid nor requires additional space for installation. Using multiple renewable resources also provides a solution for the power source problem. In that sense, it is feasible to produce hydrogen for nighttime use from surplus solar energy during the daytime. From the mutual support of the two energy sources, we can handle the shortcomings of the reserve power source/single energy use. This is the concept of a hybrid renewable energy system [1].

The solar production capacity from the household or rural production unit is relatively small, so the amount of produced hydrogen is also limited. Therefore, it is essential to use other renewable energy to run the power generator. In tropical regions, biogas is an abundant resource. In developing countries, waste from agriculture activities is the main source for producing biogas [2–3].

Using biogas as a source of cooking fuel has long been popular in rural areas of developing countries. However, if the usage of biogas is limited for this purpose only, then the consumption scale is small. A large amount of excess biogas is released into the atmosphere, affecting the environment since the greenhouse effect of methane is twenty-three times greater than CO_2. Using biogas as fuel for stationary engines and vehicle engines will expand the biogas application scope. This is a practical measure to save fossil fuel as well as mitigate global warming [4–5].

International Journal of Engineering Research & Technology (IJERT)
ISSN: 2278-0181
Vol. 9 Issue 05, May-2020

Some applications of biogas in power production and fueling agriculture machinery were put into motion [6–7]. Researches indicate the advantage of biogas as engine fuel. Supplying biogas for a stationary engine from nearby sources avoids difficulties in fuel storage and transportation. Nonetheless, studies also show some drawbacks of a biogas engine that need to be improved.

One of the main characteristics of fuel that influence the engine feature is the flammability limit and laminar flame speed [8]. Biogas contains 50%–70% methane and 30%–50% of CO_2 as well as other minor substances [9–10]. There are many studies on the effect of biogas compositions on combustion characteristics. The results showed that CO_2 in biogas narrows the flammability limit and slows down flame speed [11–13]. To improve the combustion characteristics of biogas, the addition of fuel with exceptional combustion characteristics is needed. In this perspective, hydrogen is an ideal supplement to enhance biogas engine performance. Hydrogen has high laminar flame speed, about ten times more than methane. Furthermore, it also has a larger flammability limit, which allows it to be burnt even with very poor mixtures. Thanks to these edges, the addition of hydrogen into biogas significantly improved combustion characteristics of the engines [14–16].

In the solar-biogas hybrid renewable energy system, hydrogen is both the reserve energy source for solar power as well as an additive to improve biogas combustion properties. The engine fueled with biogas-hydrogen in the system needs to meet specific criteria to operate. The traditional stationary engines in the market cannot be used for the purpose. Thus, customization is required to make these engines compatible with the hybrid energy system.

Unlike an ordinary stationary engine, in the solar-biogas hybrid renewable energy system, the generator operates in continuously changing load mode. The power control circuit of the system will start the engine when compensating load is needed. The engine power can vary in a wide range. Therefore, a flexible fuel system is required to adapt to various operating modes of the engine. Otherwise, the engine in the system must have a high level of automation to meet the requirements of the primary control.

Due to lacking this kind of engine in the market, the conversion of the traditional stationary engine into electronic control engine for the application in the solar-biogas hybrid renewable energy system is necessary. Bui et al. used a fuel injection control system used in motorbike and an opened ECU to convert a carburetor fueling engine into an electronically controlled port injection engine [17]. The advance ignition timing can be variable according to operating conditions of the engine instead of fixed position in the traditional stationary SI engine. The key features that affect the converted engine performance are the injection map and advance ignition timing map. The maps can be established primary by simulation and then adjusted by experimental data [17]. This technology is applicable in converted conventional engines into biogas-hydrogen engines used in the hybrid renewable energy system.

In this paper, the effects of operating modes and fuel composition on the performance and emission of hydrogen-enriched biogas fueling engine were studied by simulation. The study was performed on en electronic controlled engine converted from a carburetor fueling stationary engine 168FB. The simulation results are useful for mapping the fuel injection and advance ignition timing of the engine adopted in the solar-biogas hybrid renewable energy system.

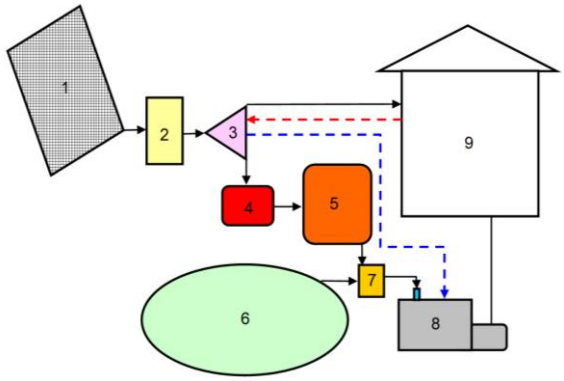

Fig. 1. The solar-biogas hybrid energy system. (1) Photovoltaic solar panel; (2) Inverter; (3) Control unit; (4) Hydrogen Electrolyser; (5) Hydrogen storage bag; (6) Biogas digester; (7) Biogas-hydrogen mixer; (8) Biogas-hydrogen generator; (9) Electrical load.

II. MATERIALS AND METHODS

A. *Materials*

The solar-biogas hybrid energy system is described in Figure 1. The control unit 3 regulates the electrical energy between the load and two power supplies: the photovoltaic (PV) solar panel 1 through the inverter 2 and the biogas-hydrogen generator 8. When the solar power is greater than the needed power for the load 9, the control 3 will transfer the surplus power into the hydrogen electrolyzer 4 to produce hydrogen. When the solar power is lower than the load power, the control unit will start the biogas-hydrogen generator 8 to compensate for the power. Hydrogen produced from the electrolyzer 4 will be stored in the storage bag 5. Biogas and hydrogen are mixed in the mixer 7 before being supplied to the engine.

The generator combining with solar energy provides the energy required by the load; therefore, the load mode changes. This is the main difference in operating mode between the engine in the hybrid energy system and a conventional stationary one. Thus, the engine of the power generator must be highly autonomous and directly controlled by the control unit. To satisfy this condition, we retrofitted a conventional 168FB engine into a biogas- hydrogen injection engine, as shown in Figure 2.

The sensors were included speed sensor, crankshaft position sensor, temperature sensor, throttle position sensor, intake airflow sensor, and oxygen sensor. They were adopted from the electronic control system of the motorcycle engine. With the information given by the sensors, the ECU to calculate the injection duration and ignition timing. Aside from that, the oxygen sensor sends feedback about the air residual coefficient so that the ECU can adjust the amount of fuel injected accordingly. It ensures the equivalent coefficient is approximately 1.

International Journal of Engineering Research & Technology (IJERT)
ISSN: 2278-0181
Vol. 9 Issue 05, May-2020

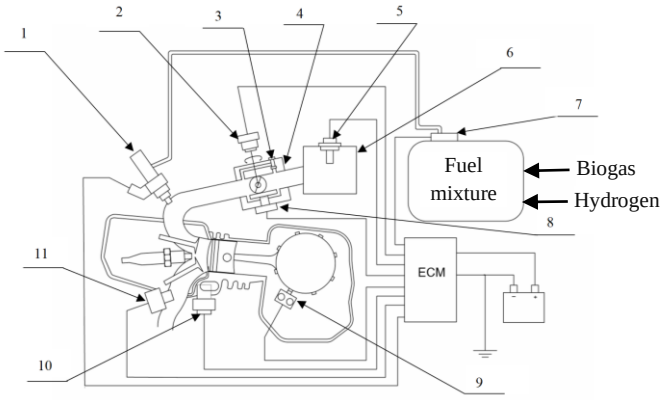

Fig. 2. Schematic diagram of fuel injection and ignition control systems of retrofitted 168FB engine. (1) Biogas-Hydrogen injector; (2) Throttle position sensor; (3) Idle air screw; (4) Throttle body; (5) Intake air temperature sensor; (6) Air filter; (7) Solenoid; (8) Idle speed control valve; (9) Crankshaft position sensor; (10) Engine oil temperature sensor; (11) Oxygen sensor.

The ECU used in the system is an opened ECU which allows the modification of the injection map and the advance ignition timing map. The 168FB engine has a 68 mm of the bore and 56 mm of stroke with a compression ratio of 8.5. When the engine is fueled with gasoline, the rated power is 4.8 kW at 3000 rpm. Figure 3 shows the cross-section of the retrofitted cylinder, combustion chamber and inlet manifold of the engine at 60 °CA.

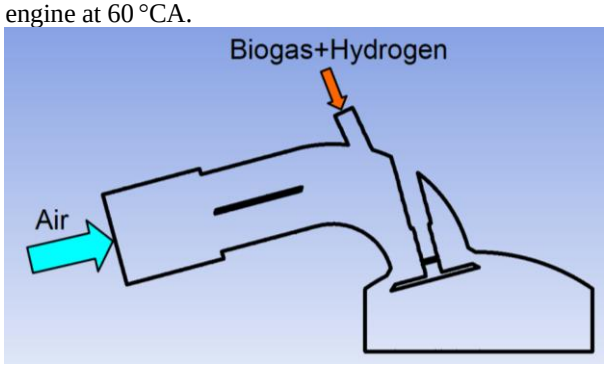

Fig. 3. The vertical cross-section of the retrofitted cylinder and intake manifold of 168FB engine

B. *Methods*

The simulation was conducted with the help of ANSYS FLUENT 18.2 CFD code. The dynamic meshing was applied for cylinder space. The intake manifold was deactivated at the closure of the admission valve of saving of calculation time. The calculation starts at the beginning of the admission stroke (0 °CA) and completes at the end of the expansion stroke (540 °CA).

The convection-diffusion equation is enclosed by k-ε model. The combustion process of the air-fuel mixture is simulated via the partially premixed combustion model. Except for NO_x concentration, the remaining substances in combustion products are in thermodynamic equilibrium. NO_x formation was determined via the Zeldovich mechanism.

The boundary conditions include air pressure and temperature at the inlet port of the intake manifold; pressure, temperature and compositions of the fuel mixture at the nozzle. Fuel compositions depend on the biogas properties and hydrogen content in the fuel mixture. The equivalence ratio is determined by the concentration of CH_4, H_2 and O_2 in the cylinder in the compression stroke.

III. RESULTS AND DISCUSSION

A. *Effects of the equivalence ratio*

Figure 4a shows the effect of the equivalence ratio to the variation of in-cylinder pressure according to the crankshaft rotation angle when the engine is fueled with biogas M7C3 enriched by 20% H_2 with an advance ignition angle of 15 °CA, operating under full load regime. In such a condition, the in-cylinder pressure reaches its maximum value when ϕ=1. Regardless of whether the mixture is rich or poor, the maximum pressure always decreases. This leads to a reduction in W_i. The mixture temperature also reaches the maximum value when ϕ=1, as shown in Figure 4b. For biogas engines, the pressure reaches its peak when the mixture is slightly rich [18–19]. When adding hydrogen into biogas, the combustion properties are improved, the maximum combustion efficiency can be obtained with the leaner mixture.

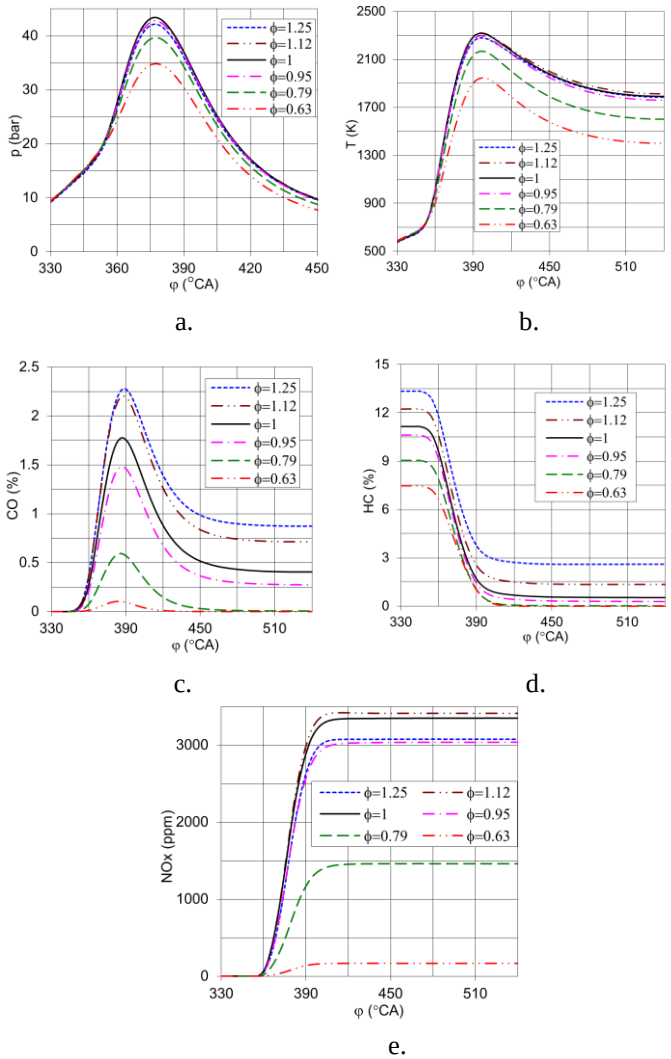

Fig. 4. Effects of the equivalence ratio on the variation of in-cylinder pressure (a), temperature (b), CO concentration (c), HC concentration (d), and NO_x concentration (e) according to the crankshaft rotation angle (M7C3, 20% H_2, n= 3000 rpm, φ_s =15°CA, 100% load)

International Journal of Engineering Research & Technology (IJERT)
ISSN: 2278-0181
Vol. 9 Issue 05, May-2020

The CO and HC concentrations greatly depend on the equivalence ratio of the mixture and the thermodynamic equilibrium. When the mixture is poor, the fuel burns completely; thus, the CO and HC concentrations are practically vanished. In theory, the combustion of a stoichiometric mixture (ϕ=1) does not produce CO and HC. However, in practice, the mixture distribution is not totally homogeneous in the combustion chamber resulting in a production of CO and HC in the local rich mixture area. Furthermore, CO in combustion products is in the equilibrium state of gas-water reaction; thus, a certain portion cannot be burned at the end of the combustion process. The CO and HC present in the combustion products is thus, even lean mixture, as shown in Figure 4c and Figure 4d. Based on the Zeldovich mechanism, the NO_x production greatly depends on the temperature, so NO_x concentration marginally varies around 3300ppm as the equivalence ratio is in the range of 0.95-1.25 (Figure 4e). NO_x concentration then drops down to 1500 ppm when ϕ=0.79, and 200 ppm when ϕ=0.63 due to the decrease of combustion temperature even larger concentration of N_2 and O_2 in poor mixture.

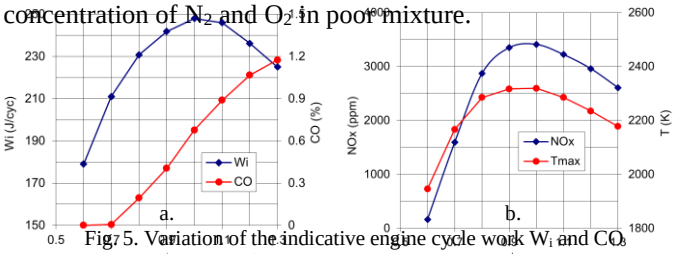

Fig. 5. Variation of the indicative engine cycle work W_i and CO concentration (a), variation of the maximum combustion temperature and NO_x concentration (b) according to the equivalence ratio (M8C2, 30%H_2, n= 3000 rpm, φ_s=20 °CA, 100% load)

Figures 5a and Figure 5b illustrate the indicative engine cycle work (W_i) and the pollutant concentrations according to the equivalence ratio. In this case, the engine running on biogas M8C2 is enriched by 30% H_2 at a speed of 3000 rpm with a fixed advance ignition angle of 20 °CA. The result shows that W_i reaches its maximum value with a stoichiometric mixture. Compare to ϕ=1, W_i decreases by 10% with ϕ=1.3 and drops by a quarter with ϕ=0.6. The CO concentration rises sharply with the equivalence ratio since the incomplete combustion prevails with the rich mixture. The variation of NO_x concentration in terms of equivalence ratio is largely like the variation of temperature.

B. Effects of the advance ignition timing

When the advance ignition angle increases, the peak of the pressure curve approaches the TDC, so the maximum value of the pressure increases together with the rise in maximum temperature (Figures 6a and Figure 6b). Figure 6a illustrates that the maximum pressure rises from 37 bar to 53 bar when the advance ignition angle expands from 10 °CA to 25 °CA. When the peak of the curve approaches the TDC, the work loss increases due to the increase of compression pressure. Therefore, the W_i does not increase proportionally to the maximum pressure. The maximum temperature rises from 2280 °K to 2360 °K when the advance ignition angle widens from 10 °CA to 25 °CA. The rise of temperature and pressure affects the formation rate of CO, leading to an increase in maximum CO concentration. However, CO concentration in the combustion products is the thermodynamic equilibrium value depending on the equivalence ratio of the mixture. It can be seen on Figure 6c, the maximum concentration of CO increases with the rising advance ignition angle, but the final CO concentration in the exhaust gas only fluctuates on an average of 0.1% when the ignition angle broadens from 10 °CA to 25 °CA.

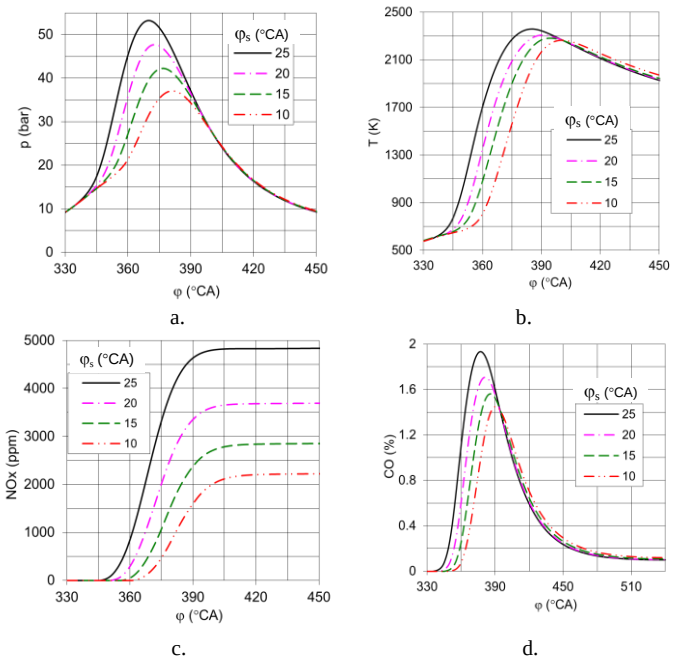

Fig. 6. Effects of the advance ignition timing on the variation of in-cylinder pressure (a), combustion temperature (b), CO concentration (c), and NO_x concentration (d) according to the crankshaft rotation angle (M6C4, 30% H_2, n= 3000 rpm, ϕ =1, 100% load)

With a given engine operation mode and fixed fuel composition, NO_x increases significantly with the advance ignition angle. This is due to the increase in temperature with the advance ignition angle. Also, the increase in combustion duration with the advance ignition timing results in a rise in NO_x concentration which is controlled by the reaction kinetics.

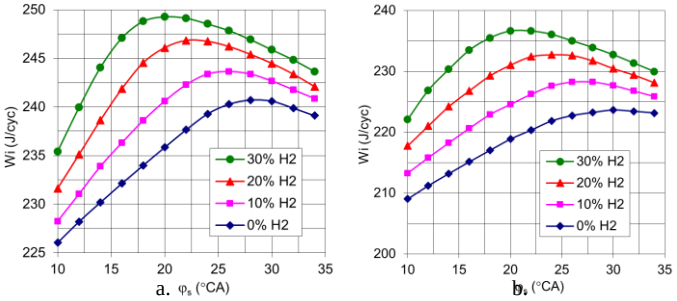

Fig. 7. Effect of hydrogen content in the fuel mixture with biogas to the variation of the indicative engine cycle work W_i according to the advance ignition angle in the case of biogas M8C2 (a) and M6C4 (b) (n=3000rpm, ϕ=1, 100% load)

Figures 7a and 7b show the effects of hydrogen content in the mixture with biogas on the variation of the indicative engine cycle work W_i according to the advance ignition angle in the case of biogas M8C2 and biogas M6C4. It can be seen that for any biogas composition or hydrogen content, the

International Journal of Engineering Research & Technology (IJERT)
ISSN: 2278-0181
Vol. 9 Issue 05, May-2020

$W_i(\varphi_s)$ curve has a peak corresponding with the optimal advance ignition angle. Since biogas contains CO_2, the laminar flame speed is lower than that of other traditional fuels. Thus, to improve combustion efficiency, the advance ignition angle of biogas engines must increase. The simulation results in Figure 7a and Figure 7b show that optimal ignition angles corresponding to M8C2 and M6C4 are 27 °CA and 30 °CA, respectively. When biogas is enriched by hydrogen, the optimal advance ignition angle is lessened due to the increase of laminar flame speed. Figure 7a reveals that the optimal advance ignition angle of the engine fueled with biogas M8C3 enriched by 10%, 20%, and 30% hydrogen is 26 °CA, 22 °CA, and 20 °CA, respectively. The optimal advance ignition angle of the engine fueled with neat biogas M8C2 is 28 °CA. Similarly, when the engine is fueled with M6C4, the optimal advance ignition angle is 27 °CA, 25 °CA, and 22 °CA corresponding with 10%, 20%, and 30% hydrogen content in the fuel mixture. The optimal advance ignition angle of the engine fueled with neat biogas M6C4 is 31 °CA. The results show that the optimal advance ignition decreases as increasing the CH_4 or/and H_2 contents in the fuel mixture.

Figure 8 indicates that for a given hydrogen content in the fuel mixture with biogas, the average optimal advance ignition angle drops by 2 °CA when the CH_4 content in biogas decreases by 20%. For a given CH_4 concentration in biogas, the reduction in optimal advance ignition angle is almost linear to the amount of hydrogen added into biogas. The slope of the curve $\varphi_s(\%H_2)$ is about 1/3 (°CA/%H_2). Thus, unlike conventional stationary SI engines, the adjustment of the advance ignition angle for the biogas-hydrogen engines in accordance with the CH_4 and H_2 content is needed to ensure effective operation.

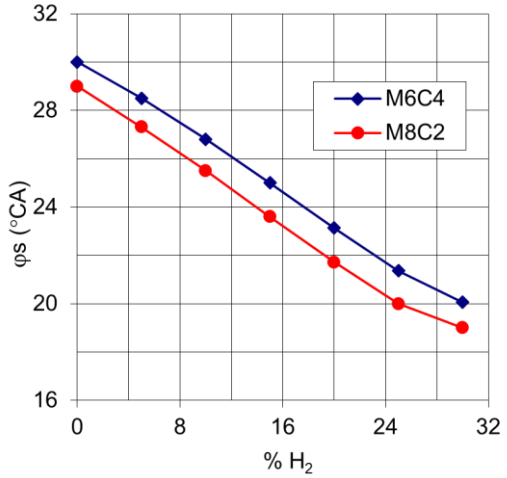

Fig. 8. Effects of biogas composition on the variation of the optimal advance ignition angle with the hydrogen content in the fuel mixture (n = 3000rpm, ϕ =1, 100% load)

The result in Figure 6c reveals that for a given fuel composition, the CO concentration in the exhaust gas only changes slightly. However, the NO_x concentration changes significantly as the result of the rise of the maximum combustion temperature when expanding the advance ignition angle. Figure 9 highlights that for the given biogas and advance ignition angle, the NO_x concentration increases with the hydrogen content in the fuel mixture. It can be observed in the figure that the NO_x concentration rises by 50% when the biogas M7C3 is enriched by 30% hydrogen regardless of the advance ignition angle. For a given biogas and hydrogen content, NO_x concentration doubles when the advance ignition angle widens from 10 °CA to 34 °CA

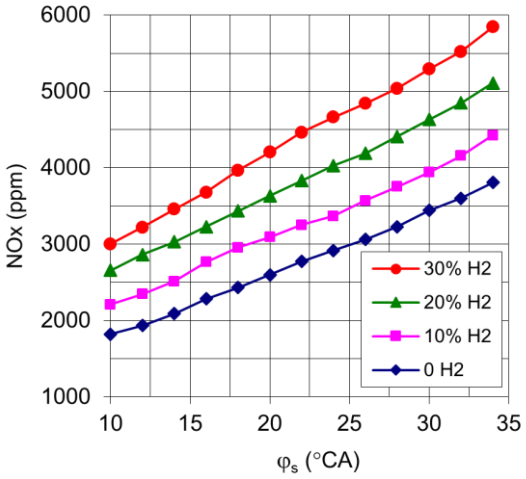

Fig. 9. Effects of hydrogen content in the fuel mixture with biogas to the variation of NO_x concentration with the advance ignition angle (M7C3, n= 3000 rpm, ϕ=1, 100% load)

When adding hydrogen into biogas, the optimal advance ignition angle reduces, and the indicative cycle work increases, as shown in Figure 7. The calculated result with M7C3 biogas indicates that the indicative engine cycle work W_i related to the optimal advance ignition angle is 233, 235, 240 and 243 J/cyc corresponding to 0%, 10%, 20% and 30% hydrogen concentration in the fuel mixture. The respective NO_x concentration in the exhaust gas in these cases only slightly fluctuates between 3900 ppm and 4000 ppm. This means when mixing 30 % hydrogen into M7C3 biogas, the indicative engine cycle work increases by 4%, while the NO_x concentration grows by 2.5%. Hence, as the engine is fueled with hydrogen-enriched biogas mixture, the advance ignition angle should be adjusted for beneficial engine cycle work while not raising pollution emission.

C. Effects of engine loading regime

Figure 10a and Figure 10b present the effects of engine loading regime to the work diagrams of the engine fueled with the neat biogas M6C4 and biogas M6C4 enriched by 30% hydrogen at 3000 rpm, ϕ=1 and the advance ignition angle φ_s=15 °CA. Comparing the results in these two figures shows that with the same throttle valve position, the maximum pressure in the case of hydrogen-enriched biogas is greater than that of the neat biogas case. The indicative cycle work corresponding to M6C4 and M6C4 enriched by 30% hydrogen is 217 and 227 J/cyc, respectively, at full load regime and is 122 and 127 J/cyc, respectively, at 50% loading regime. Thus, as shifting from neat biogas M6C4 fueling mode to biogas M6C4 enriched by 30% hydrogen fueling mode, the indicative cycle work of the engine increases by 4.6% and 4% at 100% and 50% throttle valve opening position, respectively. This means that an advance ignition angle φ_s=15 °CA is suitable with biogas M6C4 enriched by

International Journal of Engineering Research & Technology (IJERT)
ISSN: 2278-0181
Vol. 9 Issue 05, May-2020

30% hydrogen at full load regime while it is suitable with neat biogas M6C4 at 50% loading regime.

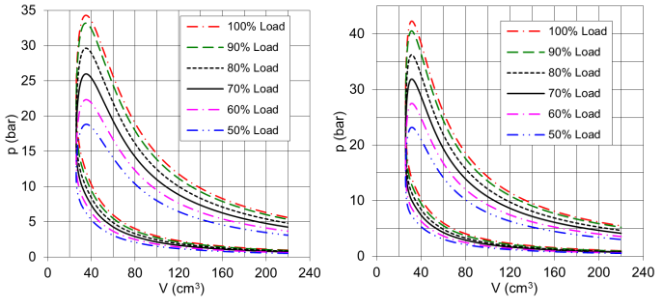

a. b.

Fig. 10. Effects of loading regime to the work diagram of the engine fueled with biogas M6C4 (a) and with biogas M6C4 enriched by 30% hydrogen (b) (ϕ=1, n=3000 rpm, φ_s=15 °CA)

Figure 11 demonstrates the variation of NO_x concentration according to the engine loading mode when the engine is fueled with biogas M6C4 and biogas M6C4 enriched by 30% hydrogen. The equivalence ratio is ϕ=1 and the advance ignition angle φ_s=15 °CA for both cases. With the given operating condition, at any loading regime, the NO_x concentration in the exhaust gas is always larger in case of hydrogen-enriched biogas fueling mode than that in case of neat biogas fueling mode. Otherwise, the NO_x concentration in the exhaust gas increases noticeably with engine loading regime. On average, the NO_x concentration goes up by 30% for M6C4 enriched by 30% hydrogen and climbs by 60% for neat M6C4 when the engine loading regime increases from 50% to 100% if the advance ignition angle is fixed at φ_s= 15 °CA.

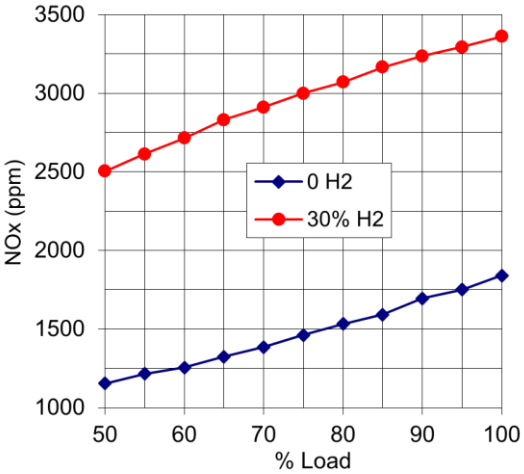

Fig. 11. Variation of NO_x in the exhaust gas corresponding with the loading regime when is fueled with biogas M6C4 and M6C4 enriched by 30% hydrogen (ϕ=1, n= 3000 rpm, φ_s=15 °CA)

When the engine is fueled with biogas-hydrogen, the optimal advance ignition angle not only changes with the fuel composition as mentioned above but also with the loading regime, as shown in Figure 12. This result indicates that as the loading regime of the engine varies from 50% to 100%, the optimal advance ignition angle varies from 19 °CA to 29 °CA with neat biogas M7C3, but it varies in narrower range from 13.5 °CA to 19 °CA with biogas M7C3 enriched by 30% hydrogen.

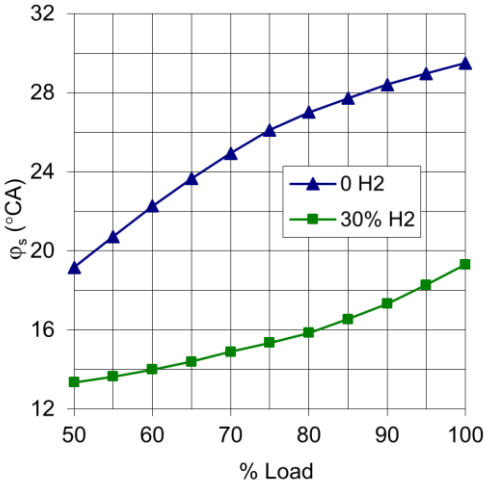

Fig. 12. Variation of optimal advance ignition angle corresponding with the engine loading mode (M7C3, ϕ=1, n=3000 rpm)

Like in full loading mode, when the engine is in partial loading mode, the NO_x concentration increases proportionally with the advance ignition angle. Figure 13 presents the variation of NO_x concentration according to the advance ignition angle when the engine runs at a 70% load regime fueled with biogas M7C3 enriched by hydrogen in different proportions. This result reveals that the NO_x level doubles when the advance ignition angle widens from 10 °CA to 34 °CA. It is similar to the case where the engine operates at 100% load fueled with hydrogen-enriched biogas that the optimal advance ignition angle drops sharply as compared to the neat biogas fueling mode. Figure 12 indicates that the engine runs at 70% load regime fueled with the neat biogas M7C3, the optimal advance ignition angle is 25 °CA, while it is 15 °CA as the engine is fueled with biogas M7C3 enriched by 30% hydrogen. If the optimal advance ignition angle is adjusted, the NO_x concentration in the exhaust gas is then 2600 ppm, and 3300 ppm as the engine is fueled with the neat M7C3 and fueled with biogas M7C3 enriched by 30% hydrogen. If the advance ignition angle is unchanged φ_s=25 °CA, the NO_x concentration in the later case is 4300 ppm.

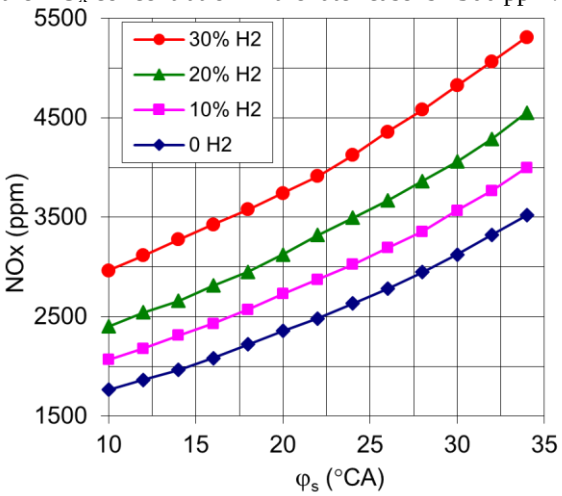

Fig. 13. Effects of the hydrogen content in the fuel mixture with biogas to the variation of NO_x concentration corresponding with the advance ignition angle (ϕ=1, n=3000 rpm)

International Journal of Engineering Research & Technology (IJERT)
ISSN: 2278-0181
Vol. 9 Issue 05, May-2020

The above results reveal that the advance ignition angle dramatically affects the performance and pollution emission of the hydrogen-enriched biogas engine. The optimal advance ignition angle varies according to the fuel composition and the loading regime of the engine. In the solar-biogas hybrid renewable energy system, the generator is responsible for compensating the electrical load; thus, the loading regime of the engine changes continuously. Besides, the hydrogen content in the mixture with biogas also changes depending on the correlation between the consumed load and the electrical power obtained from the solar PV panel. Therefore, to ensure optimal performance of the hydrogen-enriched biogas engine, an appropriate advance ignition timing map to suit the working requirements of the engine in the solar-biogas hybrid energy system is needed. This is the objective of our future studies.

IV. CONCLUSIONS

The following conclusions can be drawn from the present study:

1. The conventional stationary SI engine can be converted into an electronically controlled biogas-hydrogen fueling engine adopted to the solar-biogas hybrid renewable energy system. This is done by utilizing the fuel injection control system of a motorbike and an opened ECU to adjust the equivalence ratio and the advance ignition angle in accordance with the operating conditions and the fuel mixture compositions.

2. At a given operation regime, the indicative cycle work and NO_x concentration in the exhaust gas of the engine goes up with the increase in CH_4 or/and H_2 content in the fuel mixture. CO and HC concentrations in combustion products depend mainly on the equivalence ratio and vary within a very narrow range according to the fuel compositions.

3. With the optimal advance ignition timing, as compared to neat biogas M7C3 fueling mode, the indicative cycle work increases by 4%, while NO_x concentration rises by 2.5% as the engine is fueled with biogas M7C3 enriched by 30% hydrogen.

4. With the addition of hydrogen into biogas, the improvement of indicative cycle work is slightly moderate at partial load mode as compared to full load mode. When the engine is fueled with biogas M6C4 enriched by 30% hydrogen, the indicative cycle work goes up by 4.6% in full load mode, and by 4% in 50% load mode with a fixed advance ignition angle.

5. The optimal advance ignition angle decreases as decreasing the load regime or/and increasing the CH_4 and H_2 content in the fuel mixture. The higher advance ignition angle is, the greater NO_x concentration in the exhaust gas is.

6. In full load mode, the optimal advance ignition angle varies from 18 °CA to 29 °CA with biogas fueling mode, and from 15 °CA to 25 °CA with biogas enriched by 30% hydrogen fueling mode. In 70% load mode, the optimal advance ignition angle drops by 2 °CA compared to the full load mode with the same fueling condition.

ACKNOWLEDGEMENTS

The authors wish to express their appreciation to the Ministry of Education and Training for supporting this research through the project entitled *"Establishing models and basic parameters of the biogas-solar hybrid energy system suitable for production conditions and life in rural areas in Vietnam"*, research grant number CTB2018-DNA.04.

REFERENCES

[1] K.S. Reddy S. Aravindhan, Tapas K. Mallick, "Investigation of performance and emission characteristics of a biogas fuelled electric generator integrated with solar concentrated photovoltaic system," Renewable Energy 92 (2016) 233-243. http://dx.doi.org/10.1016/j.renene.2016.02.008

[2] Bui V.G., Tran V.N., Nguyen T.T.X., "Utilization of biogas engines in rural areas: A contribution to climate change mitigation," Colloque International RUNSUD 2010, pp. 19-31, Universite Nice-Sophia Antipolis, France, 23-25 Mars 2010

[3] Bui V.G., Tran V.N., Truong L.B.T., "Engines fueled by biogas: A contribution to energy saving and climate change mitigation," The 6th Seminar on Environment Science and Technology Issues Related to Climate Change Mitigation. Japan-Vietnam Core University Program, Osaka, Japan, 26-28 November 2008

[4] Bui V.G., Tran V.N., Le M.T., Bui T.M.T., "Combustion Analysis of Biogas Premixed Charge Diesel Dual Fuelled Engine," International Journal of Engineering Research & Technology (IJERT), Vol. 3 Issue 11, November-2014, pp. 188-194

[5] Bui V.G., Nguyen V.H., Bui T.M.T., Bui V.H., "Utilization of Poor Biogas as Fuel for Hybrid Biogas-Diesel Dual Fuel Stationary Engine," International Journal of Renewable Energy Research (Scopus), Vol. 5, No. 4, pp. 1007-1015, 2015

[6] Bui V.G., Nguyen V.D., Bui V.H., "Turbulent burning velocity in the combustion chamber of SI engine fueled with compressed biogas," Vietnam Journal of Mechanics, Volume 37, Number 3, pp 205-216, 2015

[7] Bui V.G., Bui T.M.T., "*Soot Emission Analysis in Combustion of Biogas Diesel Dual Fuel Engine,"* Environmental Science and Sustainable Development, Vol 1, No 2 (2017), pp.1-9

[8] James, L.W. Jr., Charles, C.R., Mirhd, S.S., Stephen R. H., Allen., W.W., "Handbook on Biogas Utilization," The Environment, Health, and Safety Division Georgia Tech Research Institute Atlanta, Georgia, 1988

[9] Ryckebosch E., Drouillon M., Vervaeren H., "Techniques for transformation of biogas to biomethane," Biomass and Bioenergy, Volume 35, Issue 5, May 2011, Pages 1633-1645

[10] Bond. T., and Templeton. M.R., "History and future of domestic biogas plants in the developing world," International Journal Energy for Sustainable Development Volume 15, Issue 4, pp. 347–354. 2011

[11] Hamidi N, Ilminnafik N, ING Wardana, Sabaruddin A., "An Experimental Study of the Flammability Limits of LPG-CO_2-Air Mixtures," The 2011 International Symposium on Advanced Engineering, Pukyong-Korea Proc, 2011

[12] V. Munteanu, D. Oancea, Dan Domnina Razus, "Carbon Dioxide As Inhibitor For Ignition And Flame Propagation of Propane-Air Mixtures," Analele Universitatii Bucuresti: Romania, 2002

[13] Anggono. W., Wardana. I.N.G., Lawes. M., Hughes. K.J., Wahyudi. S., Hamidi. N., "Laminar Burning Characteristics of Biogas-Air Mixtures in Spark Ignited Premix Combustion," Journal of Applied Sciences Research, 2012

[14] Bui V.G., Tran V.N., Bui T.M.T., Nguyen Q.T., "Numerical simulation studies on performance, soot and NO_x emissions of dual-fuel engine fuelled with hydrogen-enriched biogas mixtures," IET Renewable Power Generation: Volume 12, Issue 10, (2018), pp. 1111-1118, DOI: 10.1049/iet-rpg.2017.0559

[15] Bui V.G., Bui T.M.T., Truong L.B.T., Bui V.H., "Technique of Biogas-HHO Gas Supply for SI Engine," International Journal of Engineering Research & Technology (IJERT), Vol. 8 Issue 05, May-2019, pp. 669-674.

[16] Bui V.G., Bui T.M.T., Nguyen V.D., Bui V.H., "Analysis of combustion and NO_x formation in a SI engine fueled with HHO enriched biogas," Environmental Engineering and Management Journal (Accepted paper, 2020) http://www.eemj.icpm.tuiasi.ro/pdfs/accepted/58_383_Ga_19.pdf

[17] Bui V.G., Le M.T., Bui V.H., "Conversion of a conventional gasoline SI engine into electronic controlled PI engine," Journal of Science and

International Journal of Engineering Research & Technology (IJERT)
ISSN: 2278-0181
Vol. 9 Issue 05, May-2020

Technology-University of Danang, Vol.17, No11, 2019, pp. 35-41 (in Vietnamese)

[18] Bui V.G., Tran V.N., "Appropriate structural parameters of biogas SI engine converted from diesel engine," IET Renewable Power Generation, Volume: 9, Issue: 3, (2015), pp. 255-261, DOI: 10.1049/iet-rpg.2013.0329

[19] Bui V.G., Tran V.N., Le M.T., Bui T.M.T., "Combustion Analysis of Biogas Premixed Charge Diesel Dual Fuelled Engine," International Journal of Engineering Research & Technology (IJERT), Vol. 3 Issue 11, November-2014, pp. 188-194